energies

MDPI

Article

Petrology, Physical Properties and Geochemical Characteristics of Alkaline Lake Shale—Fengcheng Formation in Mahu Sag, Junggar Basin

Kang Zhao [1], Changmin Zhang [1,*], Lei Zhang [2], Zhiyuan An [2], Qinghai Xu [1] and Xinrui Zhou [1]

[1] School of Geosciences, Yangtze University, Wuhan 430100, China; 201671302@yangtzeu.edu.cn (K.Z.); qinghai.xu@yangtzeu.edu.cn (Q.X.); 2021710354@yangtzeu.edu.cn (X.Z.)
[2] Research Institute of Exploration and Development, Xinjiang Oilfield Company, PetroChina, Karamay 834000, China; zhanglei666@petrochina.com.cn (L.Z.); anzhiy@petrochina.com.cn (Z.A.)
* Correspondence: zcm@yangtzeu.edu.cn

Abstract: There are rare comparative studies on the geological characteristics of shale in different members of Permian Fengcheng Formation in Mahu Sag, Junggar basin, China. In order to compare the mineral composition, physical properties, and geochemical characteristics of shale in three members of Fengcheng Formation in Mahu Sag, a large number of test data such as X-ray diffraction, high-pressure mercury injection, organic carbon, rock pyrolysis, and vitrinite reflectance were collected and analyzed. Results showed that the content of clay minerals in the shale of the third member of Fengcheng Formation (P_1f_3) is the highest. The content of carbonate minerals is the highest and the content of clay minerals is the lowest in the shale of the second member of Fengcheng Formation (P_1f_2). The content of felsic minerals is the highest and the content of carbonate minerals is the lowest in the shale of the first member of Fengcheng Formation (P_1f_1). The physical properties of the shale of P_1f_3 are the best, and the porosity of the shale of P_1f_2 is the smallest, but its permeability is relatively large, and the permeability of shale of P_1f_1 is the lowest. The organic matter abundance of shale of P_1f_2 is the highest, while that of P_1f_1 is relatively the lowest. Most of the organic matter types of shale of P_1f_3 are type I–II, those of P_1f_2 are mainly type II, and those of P_1f_1 section are distributed from type I–III. On the whole, the shale of Fengcheng Formation in the peripheral fault zone and slope area of Mahu Sag has reached the low mature to mature stage, and the shale in the central area of the sag has reached the mature stage. More than half of the shale samples of Fengcheng Formation belong to fair to good source rocks, especially the samples of P_1f_2. A few samples from P_1f_3 and P_1f_1 belong to non-source rocks. This study indicates that the shale of Fengcheng Formation in Mahu Sag has good hydrocarbon generation potential, especially the shale of P_1f_2, and can become the target of shale oil exploration.

Keywords: mineral composition; physical properties; source rock evaluation; alkaline lake shale; Fengcheng Formation

Citation: Zhao, K.; Zhang, C.; Zhang, L.; An, Z.; Xu, Q.; Zhou, X. Petrology, Physical Properties and Geochemical Characteristics of Alkaline Lake Shale—Fengcheng Formation in Mahu Sag, Junggar Basin. *Energies* **2022**, *15*, 2959. https://doi.org/10.3390/en15082959

Academic Editor: Reza Rezaee

Received: 12 March 2022
Accepted: 15 April 2022
Published: 18 April 2022

1. Introduction

Mahu Sag is located in the northwest of Junggar basin. It is the tectonic unit with the most abundant oil and gas in Junggar basin. Many oil fields have been found in Permian, Triassic, Jurassic, and other strata, and the cumulative proved oil geological reserves exceed 20×10^9 t [1–3]. The lower Permian Fengcheng Formation source rock is the main oil supply interval of these oilfields [1–4], which shows that its oil generation capacity is very strong.

In recent years, scholars have successively agreed that Fengcheng Formation in Mahu Sag is alkaline lake deposition, and believed that it has the oldest alkaline lake high-quality source rock [5–9]. From bottom to top, Fengcheng Formation can divide into the first member of Fengcheng Formation (P_1f_1), the second member of Fengcheng Formation (P_1f_2), and the third member of Fengcheng Formation (P_1f_3) [10,11]. With the continuous advancement

of the oil and gas exploration process, a large number of oil and gas resources have been found in Fengcheng Formation [4,12–14], including shale oil, tight oil, and conventional oil reservoirs, showing the characteristics of orderly coexistence and accumulation models of conventional and unconventional hydrocarbons in Fengcheng Formation [12,14].

Predecessors have performed a lot of research on the source rocks of Fengcheng Formation [3,7,10,15–19]. However, the source rocks of Fengcheng Formation include shale, dolomite, and tuff. There are few studies on the rock mineral types, physical properties, and organic geochemical characteristics of shale. The organic matter abundance of 25 shale samples was counted by [3]. The study [15] counted and analyzed the mineral composition, pore characteristics, and total organic carbon (TOC) of dozens of shale samples from the Fengcheng Formation of the Maye 1 well. The mineral composition and micro-pore structure of 30 shale samples were described by [16]. The comparative study on the geological characteristics of shale in different members of Fengcheng Formation has been little studied. In view of this, through a number of experiments such as X-ray diffraction, high-pressure mercury injection, and geochemistry, this paper compares and analyzes the mineral composition, physical properties, organic matter abundance, organic matter type, and organic matter maturity of the shale in the three members of Fengcheng Formation, so as to clarify the differences between them.

2. Geological Setting

Junggar Basin is an important, large, superimposed petroliferous sedimentary basin in the northern part of the Xinjiang Uygur Autonomous Region, western China, and the area is approximately 13.6×10^4 km^2 [20,21]. The basin is almost triangular in shape and is wide in the south and narrow in the north. (Figure 1a,b). The basin can be divided into 6 tectonic units and 34 sub-tectonic units (Figure 1b) [22–24].

Mahu Sag is located near the northwestern margin of the basin and the northernmost secondary tectonic unit of the Central Depression, with an area of 5000 km^2 (Figure 1c) [25,26]. The west side of Mahu Sag is close to Kebai fault zone and Wuxia fault zone, the southeast side is distributed with Shiyingtan Salient, Yingxi Sag, Sangequan Salient, Xiayan Salient, and Dabasong Salient, and the southwest is connected with Zhongguai Salient (Figure 1c). Mahu Sag is one of the six major hydrocarbon-generating sags in the Junggar Basin and is also the most organic-rich hydrocarbon-generating sag in the basin [1,27]. The strata in Mahu Sag are well developed, with Carboniferous Cretaceous from bottom to top. There are four sets of source rocks (Carboniferous rocks, Jiamuhe Formation, Fengcheng Formation, and Lower Permian Wuerhe Formation), among which Fengcheng Formation is the main source rock [28,29]. Fengcheng Formation has a distribution area of about 5000 km^2 and a thickness of 50–1800 m, and is generally wedge-shaped with thickness in the West and thickness in the East.

Fengcheng Formation in Lower Permian is underlaid by the Jiamuhe Formation and overlaid by the Xiazijie Formation. The deposition of Fengcheng Formation has the characteristics of mixed deposition and complex rock types, including dolomitic rocks, clastic rocks and volcanic rocks (Figure 1d). The source rocks are mainly mudstone and dolomitic mudstone. P_1f_2 and the top of P_1f_1, and the bottom of P_1f_3 are interbedded deposits of dark shale and dolomite. Volcanic rocks of explosive facies are found in the middle and lower part of P_1f_1, and a large number of alkaline mineral deposits are found in P_1f_2. Continuous oil and gas display can be seen from the top of P_1f_1 to P_1f_3. The vertical range of oil and gas display is large, and the reservoir has the characteristics of source-reservoir in one and overall oil-bearing. The thickness of shale in P_1f_2 is the largest, followed by P_1f_3 and P_1f_1.

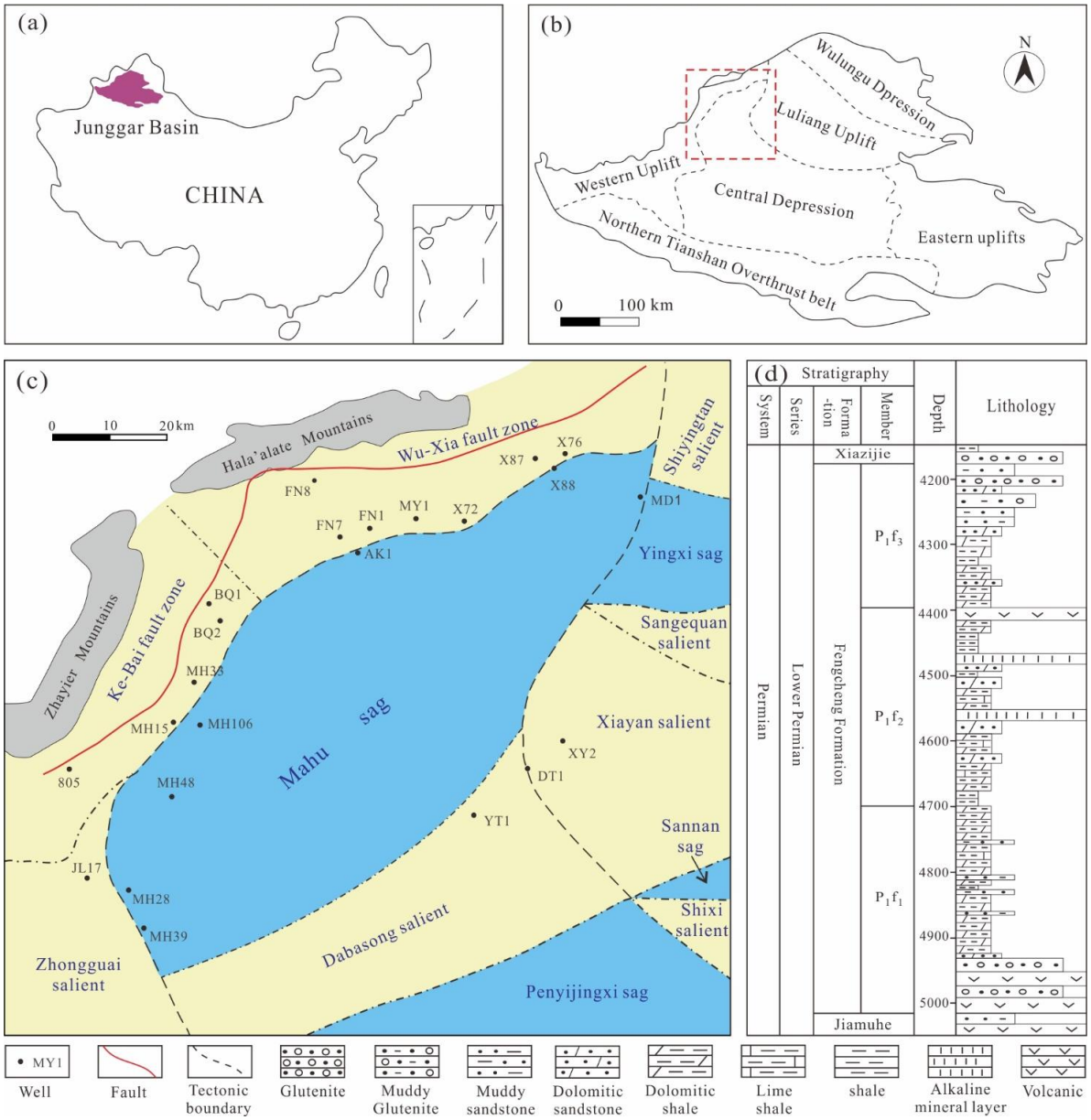

Figure 1. (**a**) Location of the Junggar Basin, China; (**b**) Division of tectonic units in the Junggar Basin and the location of the Mahu Sag; (**c**) Division of sub-tectonic units in the northwest margin of Junggar Basin; (**d**) Lithology profile of the Fengcheng Formation of well FN7 in the Mahu Sag.

3. Data and Methods

A total of 255 coring samples from 6 wells in the northwestern of Mahu Sag were collected in this paper, and the well location distribution is shown in Figure 1c. In this study, the mineral composition of shale in three members of Fengcheng Formation was identified by whole-rock X-ray diffraction analysis and rock thin section observation, in order to clarify the lithologic types of shale. According to the mercury injection experiment, the physical properties of shale were analyzed, and the porosity and permeability data were obtained. The test items including TOC, rock pyrolysis, chloroform bitumen "A", and vitrinite reflectance (Ro) were carried out on the samples in order to analyze the organic geochemical characteristics of Fengcheng Formation shale. All tests in this study were completed by the Experimental and Testing Research Institute of Xinjiang Oilfield Company, China, which is a laboratory that meets the qualifications of Chinese industry certification standards.

For the XRD analysis, the clay mineral contents of the core samples were measured using TTR XRD instrument, following SY/T5163-2010. 200 mesh powder samples were used for the whole rock mineral analysis, and the mass percentages of each mineral were calculated using analytical software and referenced to international standard sample K values. Relative mineral percentages were measured in a semi-quantitative manner. The temperature in the laboratory was 24 °C and the humidity was 35%.

For the analysis of physical properties, the core plugs were dried prior to porosity and permeability measurements with a helium porosimeter. During the measurements, a net confining pressure of 70 MPa was used to simulate formation pressure. Mercury-injected capillary pressure curves were obtained on a mercury porosimeter with the Chinese standard SY/T 5346-2005. Prior to measurement, samples were oil washed and dried to constant weight at 105 °C. The minimum intrusion pressure was set to 0.005 MPa and the maximum intrusion pressure was up to 163.84 MPa, corresponding to a pore-throat radius of approximately 4.5 nm.

For the analysis of TOC, the core samples were crushed until the particle size was less than 0.2 mm, hydrochloric acid solution was added to the container with the samples, and the temperature was controlled at 60–80 °C on an electric heating plate. After the dissolved samples were cleared of inorganic carbon for 2 h, the samples were washed with distilled water to neutral, and dried in an oven at 60–80 °C. The Chinese national standard (GB/T19145-2003) was implemented using a CS844 carbon sulfur analyzer.

For the rock pyrolysis analysis, the core was crushed to a particle size of 0.1 mm. Then, 100 mg samples were weighed, placed into Rock-Eval 6 equipment, heated to 300 °C and kept at a constant temperature for 3 min to obtain free and volatile hydrocarbon (S1), heated from 300 °C to 600 °C and kept at a constant temperature for 1 min to obtain the remaining hydrocarbon generative potential (S2), and the temperature of the maximum pyrolysis yield (T_{max}).

For the extraction of chloroform bitumen and the determination of biomarker compounds, the samples were dried and crushed to 0.18 mm, and purified chloroform was added. The heating temperature was less than 85 °C, and when the extraction solution showed no fluorescence, the extraction was completed and volatilized to dry at 40 °C, and chloroform bitumen was obtained by weighing; 0.1 mL chloroform was added to 20 mg chloroform bitumen and completely dissolved until the chloroform volatilized; then, 30 mL n-hexane was added under constant shaking, and the solution was left to rest for 12 h to precipitate asphaltenes. When the filtrate was distilled at 80 °C and concentrated to 3 mL, it was placed into a chromatography column, and 5 mL n-hexane was eluted a total of 6 times to obtain saturated hydrocarbons.

For Ro analysis, core samples were sliced and sintered with water, and then polished and placed in a drying vessel for 12 h for reflectivity measurement. The average vitrinite reflectance under oil immersion was measured using a Leica MSP200 microphotometer under green light with magnification ranging from 32 to 125 times. At a wavelength of 546 nm, Ro was obtained according to the percentage of the reflected light intensity of the vitrinite polishing surface to the vertical incident light intensity. A standard sample whose reflectivity was close to that of the sample to be tested was selected to calibrate the instrument, and then the reflection coefficient was calibrated. The number of measured points was not less than 20 and the absolute deviation was less than 0.1.

4. Results

4.1. Petrological Characteristics

The mineral composition of shale differs depending on its associated sedimentary conditions and the associated diagenetic evolutionary process [30]. The X-ray diffraction experimental analysis results of 32 shale samples of Fengcheng Formation (Figure 2a) show that the mineral types are diverse, mainly including quartz, potash feldspar, plagioclase, calcite, dolomite, clay minerals and pyrite, and the mineral content changes greatly. The shale of P_1f_3 contains quartz (20–57%, 34% on average), potash feldspar (2–10%, 5% on

average), plagioclase (5–25%, 12% on average), calcite (1–31%, 19% on average), calcite (0–27%, 11% on average), clay minerals (5–30%, 12% on average), and Pyrite (1–17%, 6% on average) (Figure 2b). The average content of dolomite in the shale of P_1f_2 is the highest, which is 30%. The average content of quartz and plagioclase are high, 27% and 22%, respectively. The maximum value of clay mineral content is 10%, the minimum value is 1%, and the average value is 6%. The average content of quartz in P_1f_1 is the highest, 37%, followed by dolomite, with an average content of 24%. The maximum value of clay mineral content is 18%, the minimum value is 4%, and the average value is 10%.

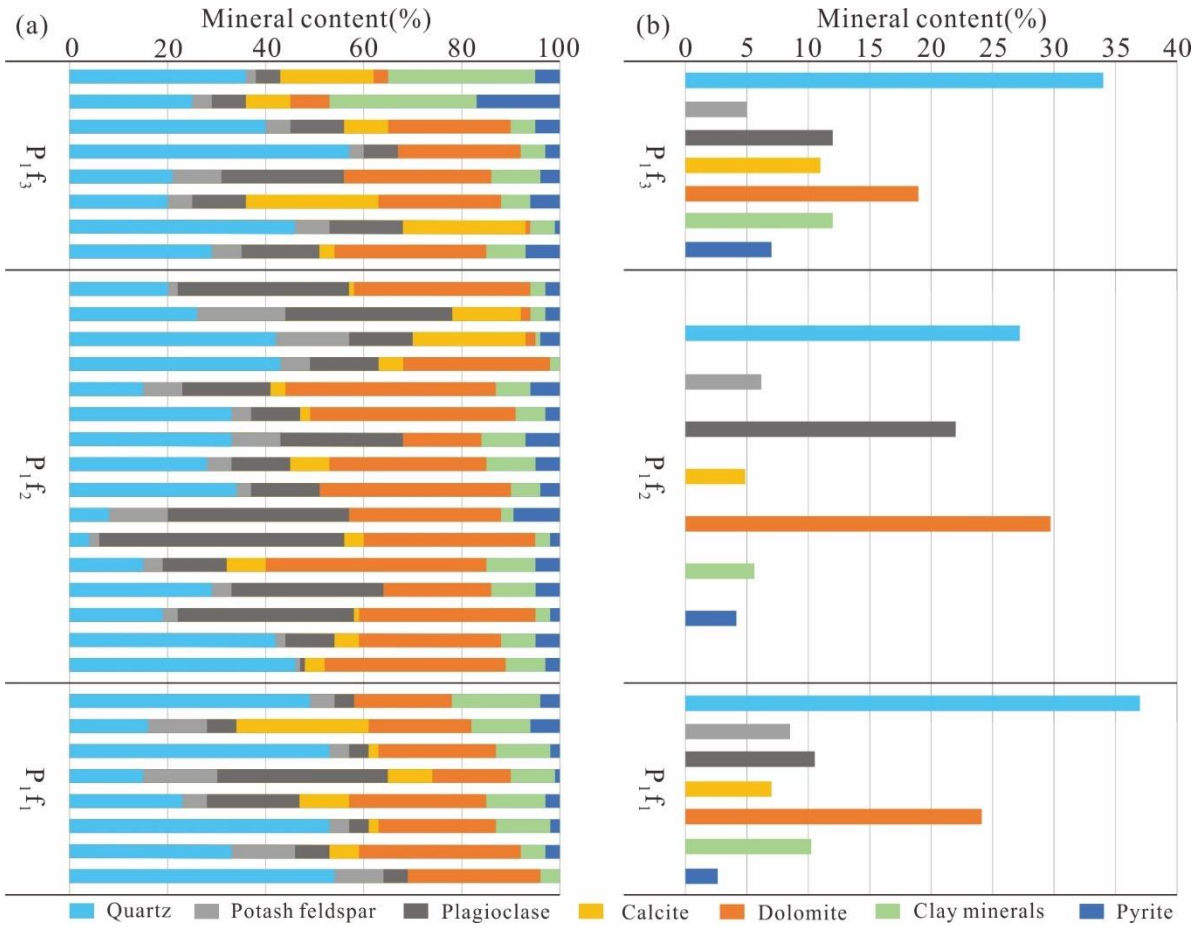

Figure 2. X-ray diffraction analysis of shale of Fengcheng Formation in Mahu Sag: (**a**) Mineral composition of each shale sample; (**b**) Mineral composition of each member.

The shale of Fengcheng Formation has the characteristics of high felsic mineral content and low clay mineral content, and the mineral composition in the shale shows obvious segmentation vertically (Figure 2b).

The clay mineral content of shale in P_1f_3 is the highest, with an average of 12% and a maximum of 30%. The dolomite content is the lowest, with an average of 12%. The clay mineral content of shale in P_1f_2 is the lowest, with an average value of 6%, and the dolomite content is the highest, with an average value of 30% and a maximum value of 45%.

At present, the classification and naming of shale are basically based on the three terminal element method. The three terminal elements are three of carbonate minerals, terrigenous clasts, clay minerals, volcanic clasts, organic matter, and other components [7,15,31–33]. In this paper, clay minerals, felsic minerals (including quartz, potash feldspar, and plagioclase), and carbonate minerals (calcite and dolomite) are used as three end elements to divide the shale of Fengcheng Formation into three types of lithofacies, namely clayey shale (zone I), felsic shale (zone II), and diamictic shale (zone III) (Figure 3). The carbonate

content in zone IV is more than 50%, mainly micritic argillaceous limestone or micritic argillaceous dolomite, which is not included in the research object of this paper.

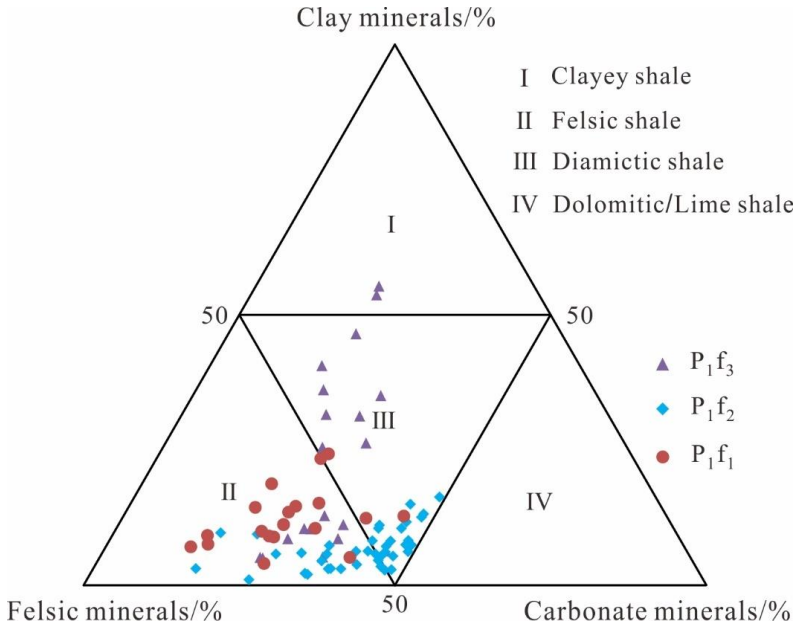

Figure 3. Rock names and classification for the shale formation of Mahu Sag.

4.2. Physical Properties

The porosity and permeability of shale in Fengcheng Formation are very small (Figure 4), indicating its poor physical properties.

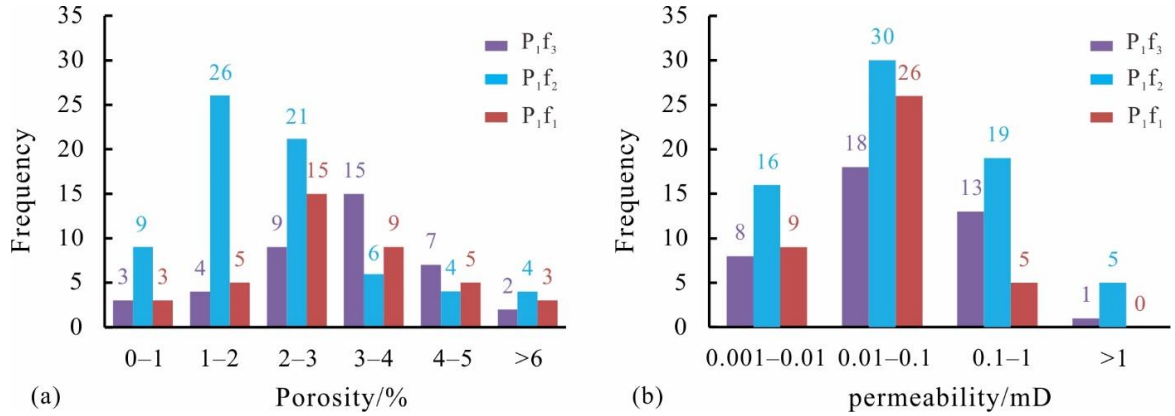

Figure 4. Frequency distribution of the physical properties of the different members in the Fengcheng Formation: (**a**) porosity; (**b**) permeability.

The physical properties values of 40 shale samples in P_1f_3 were counted. The porosity of 15 samples belongs to the range of 3–4%, accounting for about 38%. The porosity of 9 samples is in the range of 2–3%, accounting for about 23%. The porosity of 7 samples is in the range of 4–5%, accounting for about 18%. The number of samples with porosity less than 1% and porosity greater than 6 is small, only 3 samples and 2 samples, respectively (Figure 4a). The permeability of 18 samples in P_1f_3 is in the range of 0.01–0.1 mD, accounting for the most, about 45%. The second is 0.1–1 mD, with a total of 13 samples, accounting for about 33%. There is only one sample with permeability greater than 1 mD, accounting for about 3% (Figure 4b).

The physical properties values of 70 shale samples in P_1f_2 were counted. There are 30 samples with porosity of 1–2%, accounting for 43%. The porosity of 24 samples

is 2–3%, accounting for about 34%, accounting for the second. There are 10 samples with porosity less than 1%, accounting for about 14%. There are only 16 samples with porosity greater than 3%, accounting for about 23% (Figure 4a). The permeability of 30 samples is in the range of 0.01–0.1 mD, accounting for the most, accounting for about 43%. Secondly, the permeability is 0.1–1 md and 0.001–0.01 mD, accounting for about 27% and 23% respectively. There are only 5 samples with porosity greater than 1 md, accounting for about 7% (Figure 4b).

The physical properties values of 40 shale samples in P_1f_1 were counted. There are 15 samples with porosity of 2–3%, accounting for about 38%. The porosity of 9 samples is 3–4%, accounting for about 23%. The samples with porosity less than 1% and more than 6% are the smallest, with only 3, accounting for less than 8% (Figure 4a). The permeability of 26 samples is in the range of 0.01–0.1 mD, accounting for the largest proportion, accounting for about 65%. There are 9 samples with permeability of 0.001–0.01 mD, accounting for 23%. There are only 5 samples with permeability of 0.1–1 mD, and no samples with permeability greater than 1 mD (Figure 4b).

There are some differences in the physical properties of shale in different members of Fengcheng Formation. The porosity and permeability of shale in P_1f_3 are relatively the largest, and the porosity of shale in P_1f_2 is relatively the smallest (Figure 5). The minimum porosity of shale in P_1f_3 is 0.1%, the maximum porosity is 10%, the average porosity is 4%, and the main distribution range is 2–5%. The minimum porosity of shale in P_1f_2 is 0.1%, the maximum is 7.2%, the average value is 2.5%, and the main distribution range is 1–3%. The minimum porosity of shale in P_1f_1 is 0.1%, the maximum porosity is 8.6%, the average porosity is 2.8%, and the main distribution range is 2–4%. The minimum permeability of shale in P_1f_3 is 0.001 mD, the maximum permeability is 2.43 mD, the average permeability is 0.14 md, and the main distribution range is 0.02–0.2 mD. The minimum permeability of shale in P_1f_2 is 0.001 mD, the maximum is 8.7 md, the average value is 0.2 mD, and the main distribution range is 0.015–0.15 mD. The minimum permeability of shale in P_1f_1 is 0.001 mD, the maximum permeability is 0.29 mD, the average permeability is 0.07 mD, and the main distribution range is 0.01–0.1 mD. The porosity of the shale in P_1f_2 is relatively minimum, but the permeability is better than that in P_1f_1, and the maximum permeability is greater than that in P_1f_3 and P_1f_1. It is considered that the shale in P_1f_2 contains the highest content of brittle dolomite minerals. The high content of dolomite minerals leads to small shale porosity. At the same time, dolomite minerals are brittle, and dolomitic shale is prone to cracks.

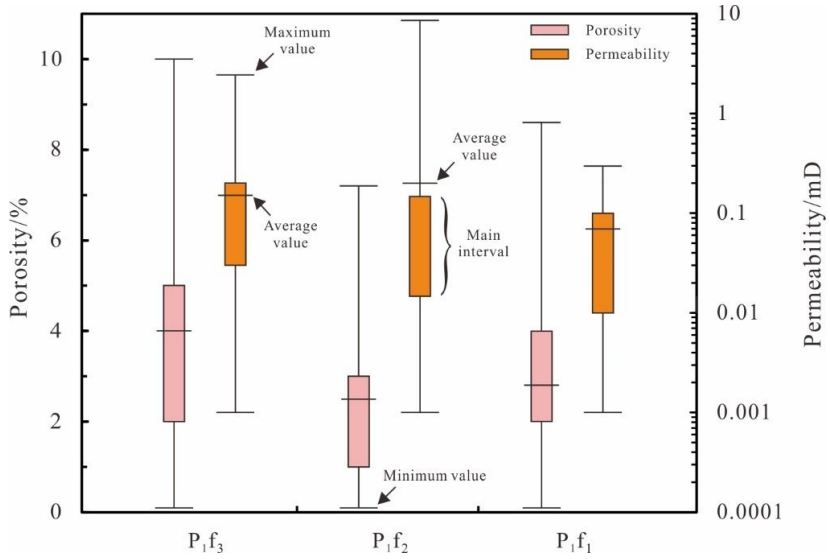

Figure 5. Distribution of porosity and permeability parameters of the Fengcheng Formation in the Mahu Sag.

4.3. Geochemical Characteristics

4.3.1. Abundance of Organic Matter

The organic matter in shale is the material basis of oil and gas generation, and the abundance of organic matter is the key to evaluate whether shale can generate a large amount of hydrocarbon. Common indicators include TOC, hydrocarbon potential generation (PG, and PG = S1 + S2), chloroform bitumen "A", and total hydrocarbon (HC) [3,7]. The geochemical characteristics of shale in the three members can be clarified separately in order to objectively evaluate the shale of Fengcheng Formation (Table 1).

Table 1. Geochemical characteristics of different members of shale in the Fengcheng Formation of the Mahu Sag.

Member	TOC (%)	PG (mg/g)	Chloroform Asphalt "A" (%)	HC (μg/g)	Tmax (°C)	HI (mg/g)	Ro (%)
P_1f_3	0.03 ~3.72 0.96(50)	0.01 ~23.29 2.09(50)	0.026 ~6.821 0.841(50)	420.26 ~6016.11 2644.42(50)	402 ~450 430.05(56)	9.83 ~900.16 389.67(56)	0.47 ~0.75 0.61(7)
P_1f_2	0.22 ~4.71 1.15(75)	0.06 ~24.58 4.00(75)	0.035 ~11.018 1.945(75)	450.12 ~6860.57 2812.40(75)	407 ~480 439.01(69)	3.17 ~802.02 274.57(69)	0.58 ~1.02 0.73(9)
P_1f_1	0.04 ~2.8 0.77(30)	0.02 ~20.1 1.83(30)	0.011 ~4.900 0.445(30)	400.45 ~5800.01 2497.68(30)	410 ~489 435.89(18)	8.04 ~799.32 284.22(18)	0.56 ~1.14 0.87(6)

$\frac{\text{minimum} \sim \text{maximum}}{\text{average(number of samples)}}$.

The TOC values of shale in P_1f_3 are 0.03–3.72%, with an average of 0.96% (Table 1). Among the 50 TOC data, 16 data are distributed in 0.7–1.4%, accounting for about 32%, accounting for the largest proportion. There are 12 data with TOC value less than 0.3%, accounting for 24% (Figure 6a). The TOC values of shale in P_1f_2 are relatively the largest, with a distribution range of 0.22–4.71%, and an average value of 1.15%. Among the TOC data of 75 shale samples in P_1f_2, 22 are distributed in 0.7–1.4%, accounting for the largest proportion, accounting for about 29%, and the data with TOC greater than 1.4%, accounting for 27%. The number of samples with TOC less than 0.3% is the least, accounting for only 11%. The TOC values of shale in P_1f_1 are relatively minimum, with a distribution range of 0.04–2.8% and an average of 0.77%; 9 of the 30 TOC data of shale in P_1f_1 are less than 0.3%, accounting for 30%, and the number of samples with TOC distribution of 0.7–1.4 is the second, accounting for 27%.

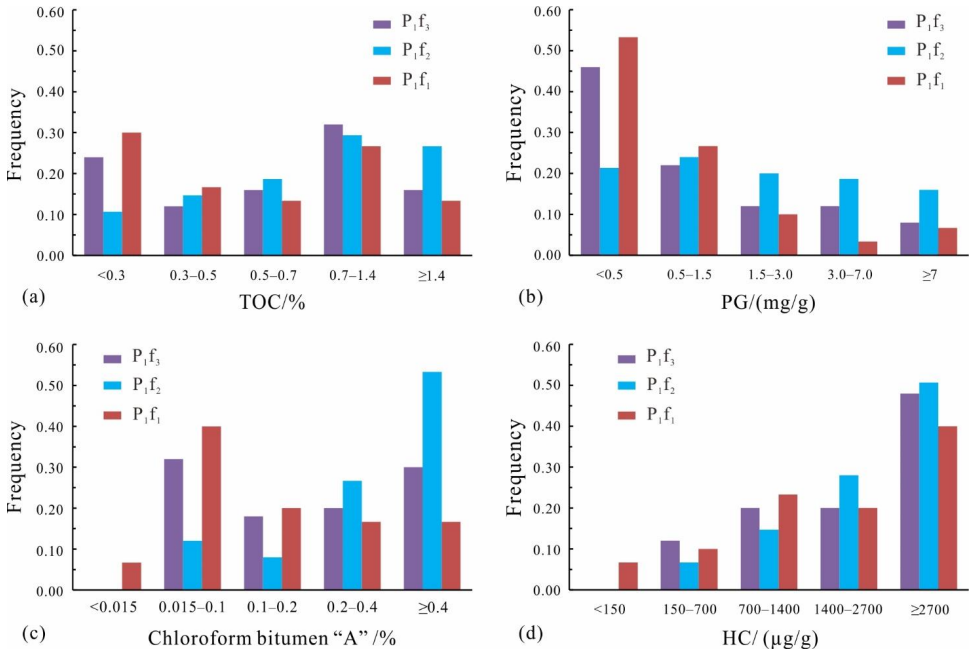

Figure 6. Distribution frequency of abundance of organic matter indicators in different members of Fengcheng Formation: (**a**) TOC; (**b**) PG; (**c**) chloroform bitumen "A"; (**d**) HC.

The PG values of shale in P_1f_2 are relatively the largest, up to 11.018 mg/g, with an average value of 1.945 mg/g, and the proportion greater than 3 mg/g reaches 35% (Figure 6b). The PG values of shale in P_1f_1 are relatively minimum, the maximum value is only 4.9%, the average value is 0.445%, and the proportion less than 0.5 mg/g is as high as 53%. Similarly, chloroform bitumen "A" and HC have the same tendency (Figure 6c,d), which shows that the values of shale in P_1f_2 are relatively the largest and the values of shale in P_1f_1 are relatively the smallest. Therefore, the organic matter abundance of shale in P_1f_2 is the highest and that of shale in P_1f_1 is relatively the lowest.

4.3.2. Type of Organic Matter

The type of organic matter largely determines the property, composition, and quantity of hydrocarbons [7,17]. This paper mainly uses the correlation diagram between the hydrogen index (HI) and T_{max} to determine the organic matter type of Fengcheng Formation shale.

The HI and T_{max} scatter plots (Figure 7) show that the organic matter types of shale samples of Fengcheng Formation are distributed from type I to type III, indicating that their organic matter sources are complex. At the same time, the organic matter types are mainly II_1, indicating that it tends to generate oil. The organic matter types of shale samples in P_1f_2 are mainly type I to type II, and the organic matter type is the best. Most of the samples are of type I to II organic shale. The distribution of organic matter types of shale samples in P_1f_1 is the most dispersed, and there is basically no dominant organic matter type. On the whole, the organic matter type of the shale in P_1f_2 is better than that in P_1f_3. The shale in P_1f_2 has stronger oil generation capacity. The organic matter type of the shale in P_1f_1 is the worst and its oil generation capacity is the worst.

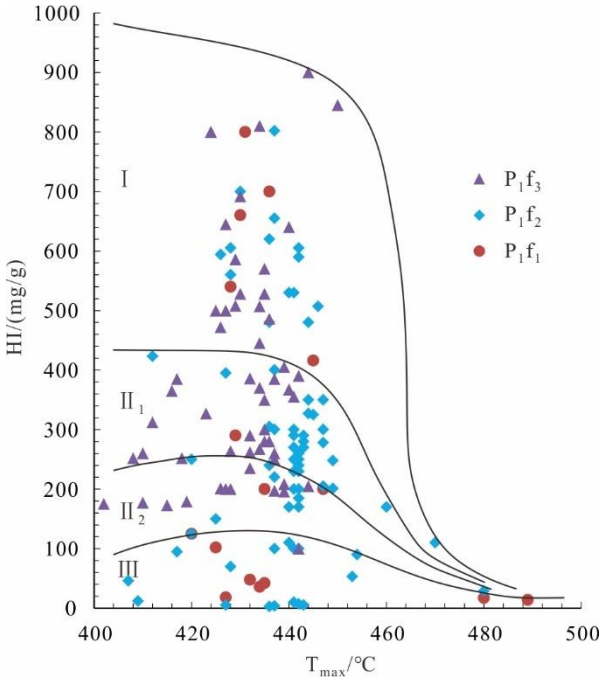

Figure 7. Scatter plot of T_{max} versus HI of different members in the Fengcheng Formation of Mahu Sag.

4.3.3. Maturity of Organic Matter

Organic matter maturity is an index to measure the degree of transformation of organic matter into oil and gas. Therefore, organic matter maturity is another important parameter for evaluating source rocks [18,19]. This study mainly uses T_{max} and Ro to measure the organic matter maturity of Fengcheng Formation shale.

The T_{max} distribution ranges of shale samples in P_1f_3, P_1f_2, and P_1f_1 are 402–450 °C, 407–480 °C, and 410–489 °C, respectively, and the average values are 430.05 °C, 439.01 °C,

and 435.89 °C, respectively (Table 1). The greater the T_{max} value, the higher the maturity of organic matter. Therefore, the shale of P_1f_3 has the lowest organic matter maturity. The shale of P_1f_2 has the highest organic matter maturity (Figure 8a). The organic matter maturity of shale in Fengcheng Formation changes greatly. The organic matter of a considerable number of samples is in the immature stage (T_{max} < 430 °C), especially the shale samples in P_1f_3. The organic matter of some samples is in the low mature stage (430 °C < T_{max} < 440 °C), and the organic matter of some samples is in the mature stage (440 °C < T_{max} < 460 °C). The organic matter of individual samples has entered a high-over mature stage (460 °C < T_{max}).

There are 23 Ro data of shale in Fengcheng Formation, including 9, 8, and 6 samples of P_1f_3, P_1f_2, and P_1f_1, respectively. The Ro distribution of shale in P_1f_3 is between 0.47–0.75%, with an average of 0.61% (Table 1). The Ro of shale in P_1f_2 is between 0.58–1.02%, with an average of 0.73%. The Ro of shale in P_1f_1 is between 0.56–1.14%, with an average of 0.87%. There are 8 samples in low mature stage (0.5 < Ro < 0.7), accounting for 35%; There are 14 samples in the mature stage (0.7 < Ro < 1.3), accounting for 61%. Only one shale sample has a Ro less than 0.5 (Figure 8b). Therefore, according to the Ro parameter, it is considered that the shale of Fengcheng Formation has generally reached the low mature to mature stage.

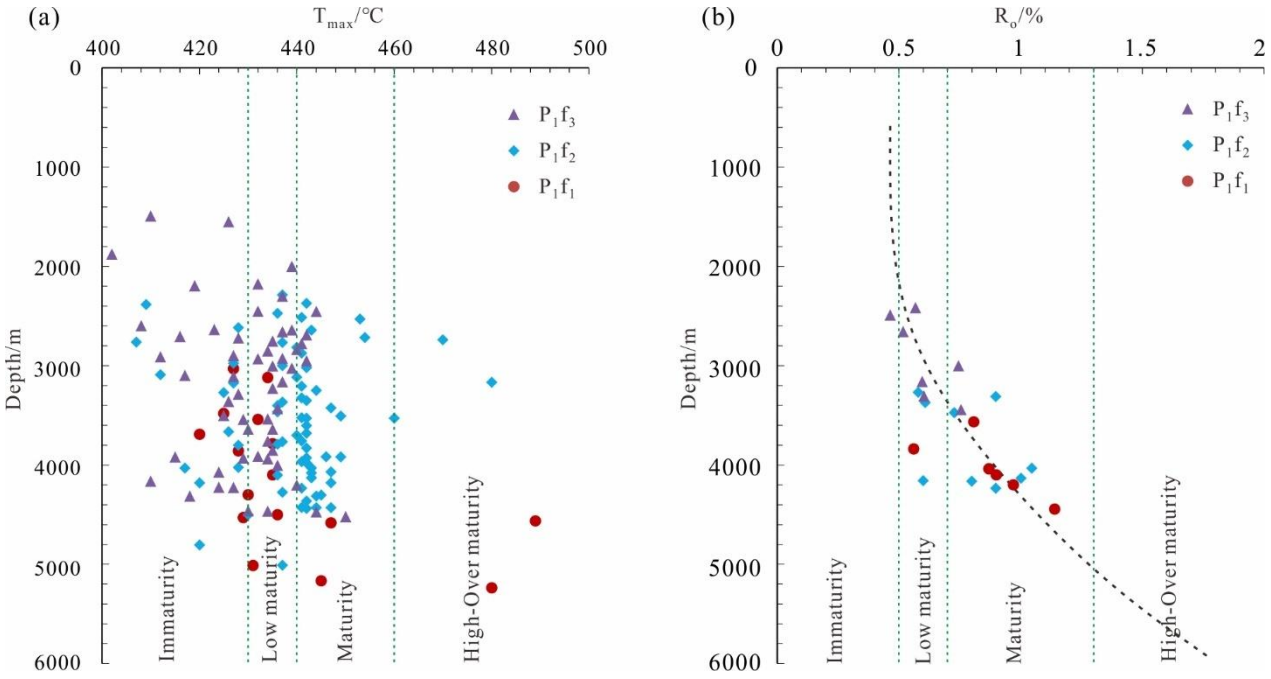

Figure 8. Variation in Maturity of organic matter indicators with depth of source rock in the Fengcheng Formation of Mahu Sag: (**a**) T_{max}; (**b**) Ro.

5. Discussion

5.1. Indication of the Content of Different Minerals

The shales of the Fengcheng Formation in the Mahu Sag are high in felsic minerals and low in clay minerals (Figure 2). It is considered that the provenance of the Fengcheng Formation is mainly from the Hala'alate Mountains, and is mostly controlled by physical weathering rather than chemical weathering. Meanwhile, due to the stronger evaporation during deposition, dolomite was developed in large quantities under quasi-syngenetic dolomitization [11,31]. The clay mineral content of shale in P_1f_3 is the highest, and the dolomite content is the lowest. It is speculated that the paleoclimate was relatively humid and cold, the lake level was high, and the water salinity was low during P_1f_3 [31]. The clay mineral content of shale in P_1f_2 is the lowest, and the dolomite content is the highest. It shows that during the deposition of P_1f_2, the climate is the driest, the lake basin shrinks, the

water salinity increases, and the calcium and magnesium ions are supersaturated, resulting in the highest mineral content of carbonate rocks [8,11].

The content of clay minerals in the shale of Fengcheng Formation in Mahu Sag is positively correlated with porosity and weakly negatively correlated with permeability (Figure 9a,b). The content of dolomite is negatively correlated with porosity and positively correlated with permeability (Figure 9b,c). This indicates that clay minerals have a positive effect on the development of shale pores, especially micro- and small pores [31,34,35]. Shales with high clay content have larger specific surface area, which is an advantage for the adsorption of shale gas [34]. Dolomite is a brittle mineral and is prone to microfractures, which can somewhat enhance the pore development [31].

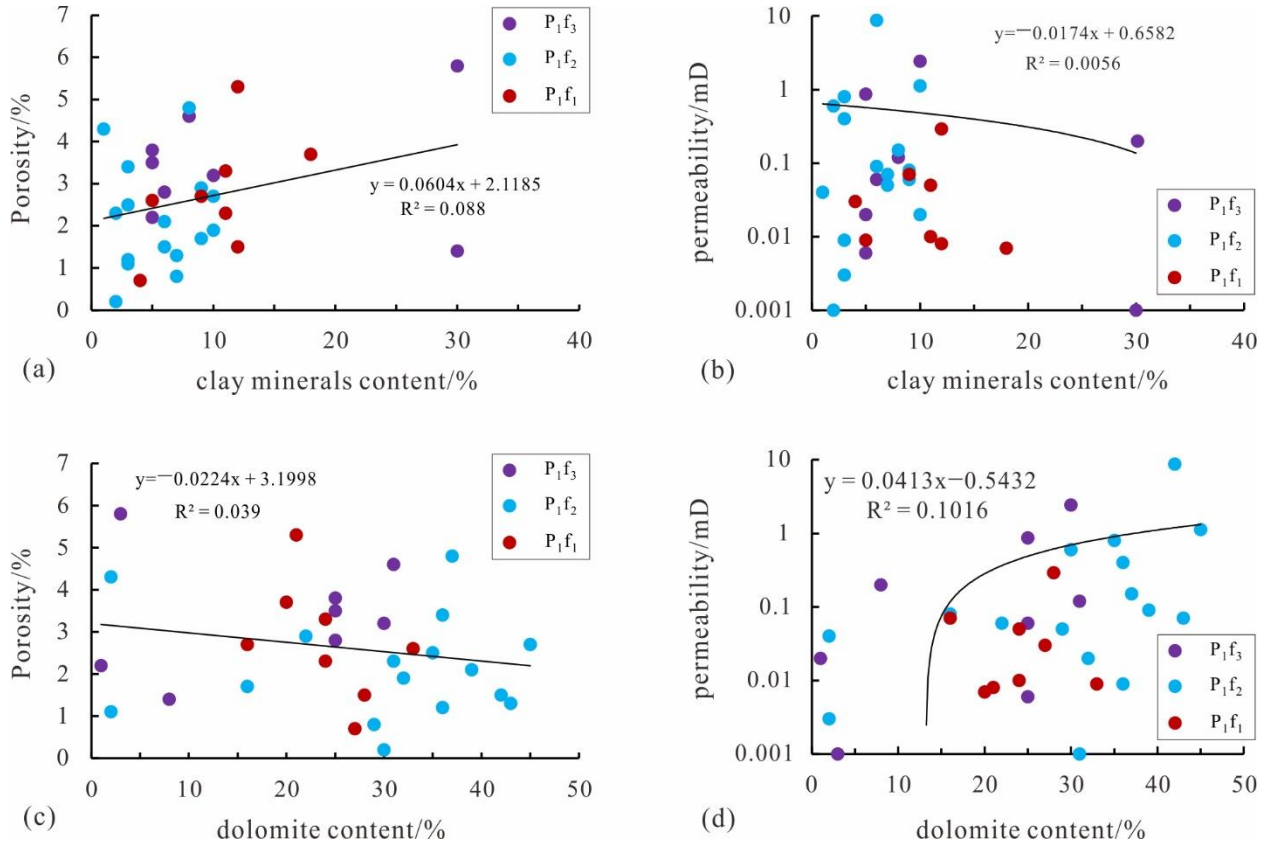

Figure 9. Relationship between mineral content and physical properties: (**a**) clay minerals content versus Porosity; (**b**) clay minerals content versus permeability; (**c**) dolomite content versus Porosity; (**d**) dolomite content versus permeability.

5.2. Comprehensive Evaluation of Source Rocks

The existing evaluation standard for terrestrial source rocks [36] is mainly for freshwater to brackish water lacustrine shale source rocks. At present, most of the documents [10,17,18,36–38] use this standard to evaluate the source rocks of Fengcheng Formation. However, the shale of Fengcheng Formation in Mahu Sag is developed under the background of alkaline lake, so it is necessary to adopt the evaluation standard suitable for alkaline lake facies source rock [19]. Study [19] evaluated the hydrocarbon generation potential of argillaceous rock, dolomite, and tuff of Fengcheng Formation. In this study, TOC, PG, and chloroform bitumen "A" are used to evaluate the hydrocarbon generation potential of shale in three members of Fengcheng Formation according to the evaluation standard of alkaline lacustrine source rock proposed in [19].

TOC and PG are used to evaluate the hydrocarbon generation potential of the shale of Fengcheng Formation (Figure 10a), which shows that more than half of the shale samples of Fengcheng Formation belong to medium to good source rocks, especially the samples of

P_1f_2. A few samples of P_1f_3 and P_1f_1 belong to non-source rocks, indicating that the shale of P_1f_2 is of the highest quality. When the TOC value is the same, the PG value of P_1f_2 is relatively the largest, and that of P_1f_1 is relatively the smallest, which indicates that the hydrocarbon generation potential of P_1f_2 shale in the study area is significantly higher than that of P_1f_3 and P_1f_1 source rocks.

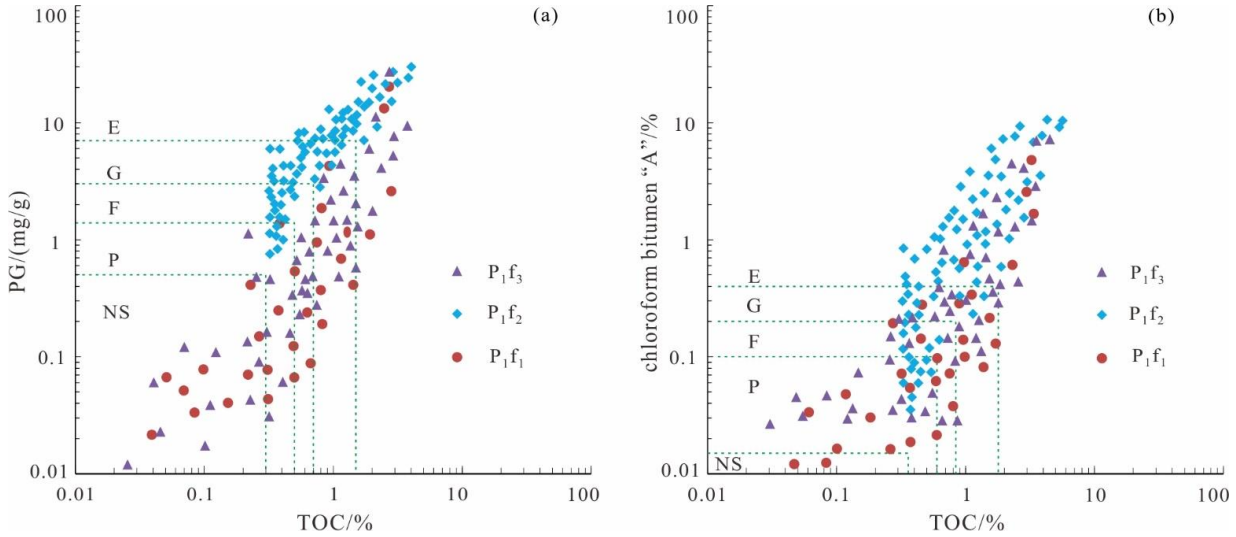

Figure 10. Source rock evaluation of the Fengcheng Formation in the Mahu Sag: (**a**) PG versus TOC; (**b**) chloroform bitumen "A" versus TOC. NS: non-source rocks; F: fair source rocks; G: good source rocks; VG: very good source rocks; E: excellent source rocks.

Using TOC and chloroform bitumen "A" to evaluate the hydrocarbon generation potential of the shale of Fengcheng Formation (Figure 10b), it shows that most of the shale samples of Fengcheng Formation belong to medium to good source rocks, and nearly half of the samples belong to good source rocks. A few samples from P_1f_3 and P_1f_1 belong to non-source rocks. With the same TOC value, the value of chloroform bitumen "A" in P_1f_2 is relatively the largest and the value of chloroform bitumen "A" in P_1f_1 is relatively the smallest, which indicates that the soluble organic matter content of shale in P_1f_2 is significantly higher than that of source rocks in P_1f_3 and P_1f_1.

5.3. Thermal Evolution History

At present, drilled wells in the study area are mainly concentrated in the high part of the structure and the slope part, relatively close to the edge of the sag (the depth is less than 5000 m), and higher quality source rocks should be more developed in the deep buried area of the sag. Therefore, based on the analysis of measured data, it is also necessary to simulate the burial thermal evolution history of source rocks in the sag.

We plotted the trend line of Ro data with buried depth (Figure 8b). With the increase of buried depth, Ro becomes larger, and there is a good correlation between buried depth and Ro, indicating that the change of Ro is mainly controlled by the normal geothermal evolution history. Therefore, the trend line can be used to predict the thermal evolution history of source rocks of Fengcheng Formation in Mahu Sag. When the burial depth reaches 2200 m, the corresponding Ro value reaches 0.5%, and the shale of Fengcheng Formation begins to enter the low mature stage. When the burial depth reaches 3400 m, the corresponding Ro value reaches 0.7%, and the shale of Fengcheng Formation begins to enter the mature stage. When the burial depth reaches 5000 m, the corresponding Ro value reaches 1.3%, and the shale of Fengcheng Formation begins to enter the high mature stage.

At the same time, based on the results of previous studies on regional geothermal distribution [39,40], the sedimentary center of Mahu Sag was selected for numerical simulation (Figure 11). The results show that Fengcheng Formation entered the hydrocarbon

generation threshold at the end of Permian and the peak of oil generation at the end of Triassic. At present, it is in the high mature stage (more than 5000 m).

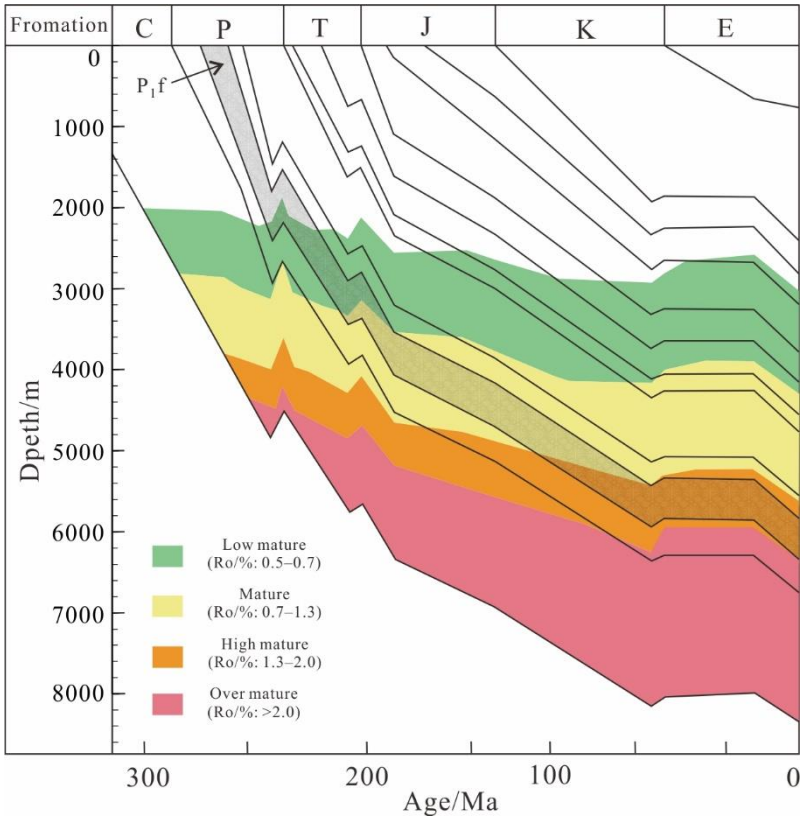

Figure 11. Burial thermal evolution history of sedimentary center in Mahu Sag.

Generally, the source rocks of Fengcheng Formation in the study area have reached the mature stage. It is speculated that the maturity increases with the increase of burial depth from slope area to sag area.

5.4. Instructions for Shale Oil Exploration

The source rocks of Fengcheng Formation in Mahu Sag are 50–400 m thick and the distribution area of high-quality source rocks is 3800 km^2 [1]. Therefore, the discovery of high-quality source rocks of Permian Fengcheng Formation in Mahu Sag not only lays an abundant material foundation for the formation of oil provinces outside the source, but also indicates that the exploration of shale oil also has great potential.

Buried depth is one of the main factors limiting the further expansion of shale oil exploration in Fengcheng Formation. However, due to the large buried depth, it has the advantage of mainly mature to high mature light oil, and the source rock can generate a certain number of gaseous hydrocarbons, which can improve the availability of crude oil. The formation pressure coefficient revealed by the drilling of Fengcheng Formation in Mahu Sag generally exceeds 1.4, up to 1.7. It gradually increases from the fault zone to the sag, which provides a great boost to the availability of shale oil [41]. Shale has high dolomite content and good brittleness, which is conducive to large-scale fracturing [32]. The content of clay minerals in P_1f_2 is high, and CO_2 gas drive can enhance production [42].

Therefore, Fengcheng Formation in Mahu Sag can become an important area for shale oil exploration. Clarifying the distribution law of "sweet spot" is the main direction of exploration at present.

6. Conclusions

The mineral composition in the shale of Fengcheng Formation shows an obvious segmentation phenomenon in the vertical direction. The content of clay minerals in P_1f_3 is the highest, with an average of 12% and a maximum of 30%. Dolomite content is the lowest, with an average of 12%. The content of clay minerals in P_1f_2 is the lowest, with an average value of 6%, and the content of dolomite is the highest, with an average value of 30% and a maximum value of 45%. The felsic content in P_1f_1 is the highest, with an average of 61% and a maximum of 79%.

The porosity and permeability of shale in Fengcheng Formation are very small, and the physical properties of shale in different sections are different. The porosity of shale in P_1f_3 is relatively the largest, with the main distribution range of 2–5%, and the permeability is relatively the largest, with the main distribution range of 0.02–0.2 mD. The porosity of shale in P_1f_2 is relatively minimum, the main distribution range is 1–3%, and the main distribution range of permeability is 0.015–0.15 mD. The main distribution range of porosity of shale in P_1f_1 is 2–4%, and the permeability is relatively minimum, with the main distribution range of 0.01–0.1 mD.

More than half of the shale samples of Fengcheng Formation belong to medium to good source rocks, especially the samples of P_1f_2. A few samples of P_1f_3 and P_1f_1 belong to non-source rocks, indicating that the shale of P_1f_2 is of the highest quality. In terms of TOC, PG, chloroform bitumen "A", and HC, the value of P_1f_2 is relatively the largest and that of P_1f_1 is relatively the smallest, indicating that the organic matter abundance of shale in P_1f_2 is the highest and that of shale in P_1f_1 is relatively the lowest.

The source of organic matter in the shale of Fengcheng Formation is complex. The types of organic matter are distributed from type I to type III, mainly type II_1. The organic matter type of the shale in P_1f_2 is better than that in P_1f_3. The shale in P_1f_2 has stronger oil generation capacity. The organic matter type of P_1f_1 is the worst and its oil generation capacity is the worst.

The shale of Fengcheng Formation in the peripheral area of Mahu Sag has generally reached the low mature to mature stage. Towards the direction of sag, the maturity of organic matter increases with the increase of burial depth, and has generally reached the high mature stage.

Author Contributions: Conceptualization, C.Z. and K.Z.; methodology, C.Z.; software, K.Z.; validation, L.Z., Z.A., Q.X. and X.Z.; investigation, K.Z.; resources, L.Z. and Z.A.; data curation, K.Z., L.Z. and Z.A.; writing—original draft preparation, K.Z.; writing—review and editing, C.Z.; supervision, Q.X.; project administration, C.Z.; funding acquisition, C.Z. All authors have read and agreed to the published version of the manuscript.

Funding: This research was funded by the National Natural Science Foundation of China, grant number 42130813 and CNPC Innovation Found, grant number 2021DQ02-0106.

Institutional Review Board Statement: Not applicable.

Informed Consent Statement: Not applicable.

Data Availability Statement: Not applicable.

Acknowledgments: We thank the Research Institute of Petroleum Exploration and Development, PetroChina Xinjiang Oilfield, for allowing us to access their database, providing background geologic data, and allowing us to publish the results.

Conflicts of Interest: The authors declare no conflict of interest.

References

1. Lei, D.; Chen, G.; Liu, H.; Li, X.; Albumint, T.K.; Cao, J. Study on the forming conditions and exploration fields of the Mahu giant oil(gas)province, Junggar Basin. *Acta Geol. Sin.* **2017**, *91*, 1604–1619.
2. Zhao, W.; Hu, S.; Guo, X.; Li, J.; Cao, Z. New concepts for deepening hydrocarbon exploration and their application effects in the Junggar Basin, NW China. *Petrol. Explor. Dev.* **2019**, *46*, 811–819. [CrossRef]

3. Liu, D.; Zhou, L.; Li, S.; Ma, W.; Guo, W. Characteristics of source rocks and hydrocarbon generation models of Fengcheng Formation in Mahu Depression. *Acta Sedimentol. Sin.* **2020**, *38*, 946–955.
4. Zhi, D.; Tang, Y.; He, W.; Guo, X.; Zheng, M.; Huang, L. Orderly coexistence and accumulation models of conventional and unconventional hydrocarbons in Lower Permian Fengcheng Formation, Mahu Sag, Junggar Basin. *Petrol. Explor. Dev.* **2021**, *48*, 43–59. [CrossRef]
5. Zhi, D.; Cao, J.; Xiang, B.; Qin, Z.; Wang, T. Fengcheng alkaline lacustrine source rocks of Lower Permian in Mahu Sag in Junggar Basin: Hydrocarbon generation mechanism and petroleum resources reestimation. *Xinjiang Pet. Geol.* **2016**, *37*, 499–506.
6. Gao, G.; Yang, S.; Ren, J.; Zhang, W.; Xiang, B. Geochemistry and depositional conditions of the carbonate-bearing lacustrine source rocks: A case study from the Early Permian Fengcheng Formation of Well FN7 in the northwestern Junggar Basin. *J. Pet. Sci. Eng.* **2018**, *162*, 407–418. [CrossRef]
7. Wang, X.; Wang, T.; Cao, J. Basic characteristics and highly efficient hydrocarbon generation of alkaline-lacustrine source rocks in Fengcheng Formation of Mahu Sag. *Xinjiang Pet. Geol.* **2018**, *39*, 9–15.
8. Cao, J.; Xia, L.; Wang, T.; Zhi, D.; Tang, Y.; Li, W. An alkaline lake in the Late Paleozoic Ice Age (LPIA): A review and new insights into paleoenvironment and petroleum geology. *Earth-Sci. Rev.* **2020**, *202*, 103091. [CrossRef]
9. Wang, T.; Cao, J.; Jin, J.; Xia, L.; Xiang, B.; Ma, W. Spatiotemporal evolution of a Late Paleozoic alkaline lake in the Junggar Basin, China. *Mar. Pet. Geol.* **2020**, *124*, 104799. [CrossRef]
10. Hu, T.; Pang, X.; Yu, S.; Wang, X.; Pang, H.; Guo, J.; Jiang, F.; Shen, W.; Wang, Q.; Xu, J. Hydrocarbon generation and expulsion characteristics of Lower Permian P_1f source rocks in the Fengcheng area, northwest margin, Junggar Basin, NW China: Implications for tight oil accumulation potential assessment. *Geol. J.* **2016**, *51*, 880–900. [CrossRef]
11. Qi, W.; Wu, J.; Xia, Y.; Zhang, X.; Li, Z.; Chang, J.; Bai, J. Influence of ionic composition on minerals and source rocks: An investigation between carbonate-type and sulfate-type lacustrine sediments based on hydrochemical classification. *Mar. Pet. Geol.* **2021**, *130*, 105099. [CrossRef]
12. Zou, C.; Zhi, Y.; Zhang, G.; Hou, L.; Zhu, R.; Tao, S.; Yuan, X.; Dong, D.; Wang, Y. Conventional and unconventional petroleum "orderly accumulation": Concept and practical significance. *Petrol. Explor. Dev.* **2014**, *41*, 14–27. [CrossRef]
13. Li, X.; Zhang, K.; Lin, H.; Zhang, G.; Hou, D. Reservoir characterization and hydrocarbon enrichment factors of the Permian Fengcheng Formation in the northwestern margin of Junggar Basin. *Spec. Oil Gas Reserv.* **2019**, *26*, 37–44.
14. He, W.; Qian, Y.; Zhao, Y.; Li, N.; Zhao, Z.; Liu, G.; Miao, G. Exploration lmplications of Total Petroleum System in Fengcheng Formation, Mahu Sag, Junggar Basin. *Xinjiang Pet. Geol.* **2021**, *42*, 641–655.
15. Yang, F.; Meng, X.; Wang, X.; Yu, P.; Shao, G.; Chen, H. Micro-Pore characteristics and influencing factors of Fengcheng Formation shale in well Maye-1. *Xinjiang Pet. Geol.* **2022**, *43*, 1–10.
16. Yang, Z.; Tang, Y.; Guo, X.; Huang, L.; Wang, Z.; Zhao, X. Occurrence states and potential influencing factors of shale oil in the Permian Fengcheng Formation of Mahu Sag, Junggar Basin. *Pet. Geol. Exp.* **2021**, *43*, 784–796.
17. You, X.; Gao, G.; Wu, J.; Zhao, J.; Liu, S.; Duan, Y. Differences of effectivity and geochemical characteristics of the Fengcheng Formation source rock in Ma'nan area of the Junggar Basin. *Nat. Gas Geosci.* **2021**, *32*, 1697–1708.
18. Qin, Z.; Zhi, D.; Xi, K. Organic petrology, geochemistry, and hydrocarbon generation capacity of Permo-Carboniferous source rocks in the Mahu Sag, northwestern Junggar Basin, China. *Energy Explor. Exploit.* **2022**, *40*, 57–78. [CrossRef]
19. Tang, Y.; He, W.; Bai, Y.; Zhang, X.; Zhao, J.; Yang, S.; Wu, H.; Zou, Y.; Wu, W. Source rock evaluation and hydrocarbon generation model of a Permian alkaline lakes—a case study of the Fengcheng Formation in the Mahu Sag, Junggar Basin. *Minerals* **2021**, *11*, 644. [CrossRef]
20. Sun, K.; Chen, Q.; Chen, G.; Chen, C. Quantitative analysis of amorphous silica and its influence on reservoir properties: A case study on the shale strata of the Lucaogou Formation in the Jimsar Depression, Junggar Basin, China. *Energies* **2020**, *13*, 6168. [CrossRef]
21. Yu, K.; Zhang, Z.; Cao, Y.; Qiu, Y.; Yang, Y. Origin of biogenic-induced cherts from Permian alkaline saline lake deposits in the NW Junggar Basin, NW China: Implications for hydrocarbon exploration. *J. Asian Earth Sci.* **2021**, *211*, 104712. [CrossRef]
22. Zhu, D.; Liu, X.; Guo, S. Reservoir formation model and main controlling factors of the carboniferous volcanic reservoir in the Hong-Che Fault Zone, Junggar Basin. *Energies* **2020**, *13*, 6114. [CrossRef]
23. Wang, S.; Wang, G.; Huang, L.; Song, L.; Zhang, Y.; Li, D. Logging evaluation of lamina structure and reservoir quality in shale oil reservoir of Fengcheng Formation in Mahu Sag, China. *Mar. Pet. Geol.* **2021**, *133*, 105299. [CrossRef]
24. Chen, Z.; Wang, X.; Zha, M.; Zhang, Y.; Cao, Y.; Yang, D.; Wu, K.; Chen, Y. Characteristics and formation mechanisms of large volcanic rock oil reservoirs: A case study of the carboniferous rocks in the Kebai fault zone of Junggar Basin China. *AAPG Bull.* **2016**, *100*, 1585–1617. [CrossRef]
25. Bian, W.; Hornung, J.; Liu, Z.; Wang, P.; Hinderer, M. Sedimentary and palaeoenvironmental evolution of the Junggar basin, Xinjiang, northwest China. *Palaeobiodivers. Palaeoenviron.* **2010**, *90*, 175–186. [CrossRef]
26. Chen, Z.; Zha, M.; Liu, K.; Zhang, Y.; Yang, D.; Tang, Y.; Wu, K.; Chen, Y. Origin and accumulation mechanisms of petroleum in the carboniferous volcanic rocks of the Kebai Fault Zone, western Junggar Basin, China. *J. Asian Earth Sci.* **2016**, *127*, 170–196. [CrossRef]
27. Tang, Y.; Guo, W.J.; Wang, X. A new breakthrough in exploration of large conglomerate oil province in Mahu Sag and itsimplications. *Xinjiang Pet. Geol.* **2019**, *40*, 127–137.

28. Yu, K.; Cao, Y.; Qiu, L.; Sun, P. The hydrocarbon generation potential and migration in an alkaline evaporite basin: The Early Permian Fengcheng Formation in the Junggar Basin, northwestern China. *Mar. Pet. Geol.* **2018**, *98*, 12–32. [CrossRef]
29. Feng, C.; Ma, M.; He, W.; Li, T.; Wu, Q.; Zhang, Z.; Zhao, H. Paleoenvironmental changes of source rocks from the Carboniferous to Permian sediments of the Mahu Sag, Junggar Basin, China. *Geosystem Eng.* **2020**, *23*, 276–286. [CrossRef]
30. Wang, X.; Liu, Y.; Hou, J.; Li, S.; Kang, Q.; Sun, S.; Ji, L.; Sun, J.; Ma, R. The relationship between synsedimentary fault activity and reservoir quality—A case study of the Ek1 Formation in the Wang Guantun area, China. *Interpretation* **2020**, *8*, 15–24. [CrossRef]
31. Zhang, Y.; Wang, G.; Song, L.; Bao, M.; Huang, Y.; Lai, J.; Wang, S.; Huang, L. A logging identification method of shale lithofacies: A study of Fengcheng Formation in Mahu Sag, Junggar Basin. *Prog. Geophys.* **2022**, *1*, 1–16.
32. Xi, K.; Cao, Y.; Zhu, R.; Shao, Y.; Xue, X.; Wang, X.; Gao, Y.; Zhang, J. Rock types and characteristics of tight oil reservoir in Permian Lucaogou Formation, Jimsar sag. *Acta Pet. Sin.* **2015**, *36*, 1495–1507.
33. Xiong, F.; Jiang, Z.; Huang, H.; Wen, M.; Moortgat, J. Mineralogy and gas content of Upper Paleozoic Shanxi and Benxi Shale Formations in the Ordos Basin. *Energy Fuels.* **2019**, *3*, 1061–1068. [CrossRef]
34. Wang, X.; Hou, J.; Li, S.; Dou, L.; Song, S.; Kang, Q.; Wang, D. Insight into the nanoscale pore structure of organic-rich shales in the Bakken Formation, USA. *J. Petrol. Sci. Eng.* **2019**, *176*, 312–320. [CrossRef]
35. Wang, X.; Zhou, X.; Li, S.; Zhang, N.; Ji, L.; Lu, H. Mechanism study of hydrocarbon differential distribution controlled by the activity of growing faults in faulted basins: A case study of paleogene in the Wang Guantun Area, Bohai Bay Basin, China. *Lithosphere* **2021**, *2021*, 7115985. [CrossRef]
36. Huang, F.; Xin, M. *Geochemical Evaluation Method of Nonmarine Source Rocks*; China National Petroleum Corporation: Beijing, China, 1995.
37. Li, S.; Hu, S.; Sun, M. *Analysis and Comprehensive Evaluation of Source Rock Characteristics in Hydrocarbon Rich Depressions in Eastern China*; China University of Geosciences Press: Wuhan, China, 2016.
38. Zhi, D.; Song, Y.; He, W.; Jia, X.; Huang, L. Geological characteristics, resource potential and exploration direction of Middle Lower Permian shale oil in Junggar Basin. *Xinjiang Pet. Geol.* **2019**, *40*, 389–401.
39. Qiu, N.; Wang, X.; Yang, H.; Xiang, Y. The characteristics of temperature distribution in the Junggar basin. *Chin. J. Geol.* **2001**, *36*, 350–358.
40. Qiu, N.; Yang, H.; Wang, X. Tectonic-thermal evolution in the Junggar basin. *Chin. J. Geol.* **2002**, *37*, 423–429.
41. Zhi, D.; Tang, Y.; Zheng, M.; Xu, Y.; Cao, J.; Ding, J.; Zhao, Y. Geological characteristics and accumulation controlling factors of shale reservoirs in Fengcheng Formation, Mahu Sag, Junggar Basin. *China Pet. Explor.* **2019**, *24*, 650–658.
42. Zhang, C.; Ranjith, P.G.; Mandadige, P.; Zhao, J. Characteristics of clay-abundant shale formations: Use of CO_2 for production enhancement. *Energies* **2017**, *10*, 1887. [CrossRef]